Project Alshain: A Lunar Flying Vehicle for Rapid Universal Surface Access

University of Maryland, College Park
ENAE484: Space Systems Design

Faculty Advisors
Dr. David Akin
Dr. Mary Bowden

Student Leads
Sarah Beal
Nick D'Amour
Adam Halperin
Alex Janas
Breanne McNerney
Nitin Sydney

Submission Date: 5/14/2009

List of Student Team Members

* All team members are senior undergraduates

Sarah Beal
Nicolas D'Amore
Patik Dave
Amirhadi Ekrami
Edwin Fernandes
Adam Halperin
Bryan Han
Alex Janas
Adam Kirk
Matthew Kosmer
Ryan Lebois
Arber Masati
Andrew McLaren
Breanne McNerney
Zachary Neumann
Nathaniel Niles
Joseph Park
Kush Patel
Fazle Siddique
Michael Sotak
Nitin Sydney
Theodor Talvac
Andrew Turner
Neal Vasilak
Scott Weinberg
Andrew Wilson
Jarred Young
Jolyon Zook

Abstract

This document presents the results of a design study investigating the concept of a lunar flying vehicle. Project Alshain (Arabic for "falcon") promises to dramatically augment the capabilities of NASA's Project Constellation by providing rapid access to remote regions, isolated from the lunar outpost by distance or terrain. The lunar equivalent of a helicopter as already in use for Antarctic exploration, Alshain is a natural supplement to the ground-based exploration architecture currently envisioned for the moon. As designed, the vehicle supports a nominal sortie with two suited astronauts of up to 57 km in range and 8 hours in duration, enabling exploration of previously inaccessible locations on mountains and in rilles and craters.

Delivered to the moon on an unmanned Altair cargo delivery mission, the vehicle will supplement exploration efforts centered from the planned south pole outpost. To improve the economic feasibility of this endeavor, the vehicle has been designed to make use of liquid hydrogen and liquid oxygen propellants produced in situ from mined water ice, thus avoiding the costly process of transporting propellants to the moon. This propellant will be used for both a central main engine and reaction control thrusters, fed by a pressurized Helium system.

The vehicle will nominally follow a modified ballistic trajectory, transporting the crew and up to 170 kg of cargo as far as 57 km in less than six minutes. Constant-altitude propulsive glides are an additional option to improve crew sightlines for shorter traverses. These flights can be controlled directly by the crew, remotely in teleoperation, or autonomously by the onboard computers.

Introduction

Since the Apollo program, the United States has foregone going to the Moon in order to focus on other space applications. However, with the advent of the Constellation Program, NASA plans a triumphant manned return to the moon, and the establishment of a permanent lunar base near the south pole. One goal of the base is to further exploration and research of the lunar surface.

With the installation of a permanent outpost, a transportation infrastructure must be developed in order to efficiently travel, research, and explore the Moon's surface. Since a permanent outpost has never been developed, one can use the Antarctic base infrastructure as an analogue to what means of transportation must be made available in such an uninhabitable, unexplored environment. For example, in Antarctica, scientists have the means to travel short distances between buildings and around the base using snowmobiles, and the ability to conduct longer research missions using closed cabin vehicles. The use of helicopters and aircraft enables unsurpassed range and speed for long distance missions. Similarly, unpressurized rovers could be the snowmobiles of the lunar base, while pressurized rovers are able to conduct missions that are both longer and farther away. However, the means to travel long distances quickly and reach inaccessible areas has yet to be explored in-depth. Thus, a lunar flying vehicle (LFV) has been proposed to accomplish these tasks and supplement the South Pole base transportation infrastructure.

A lunar flying vehicle provides extraordinary potential as a means of transportation on the Moon. Such benefits include access to sites otherwise inaccessible to a lunar rover, including rilles, craters, mountains, and potential lava tubes. To cite a past NASA example, Apollo 15 landed next to Hadley Rille, but was with no means to traverse the slope of the rille, it was left unexplored. An LFV also provides a means of quickly reaching any damaged or broken vehicles, such as a rover, in order to perform crew rescue operations. The unparalleled speed and mobility provided by an LFV make it an ideal choice to supplement lunar exploration.

The concept of a Lunar Flying Vehicle has not been given serious consideration since the late 1960s, and the Apollo program. During this time, several LFV designs were proposed to be used not only for exploration, but some were intended for a contingency return of astronauts to lunar orbit. Designs included the North American company's LFV which was a short range vehicle intended to carry a single astronaut and cargo a distance of up to 8.5 kilometers. This design continued through to a preliminary design review but was cancelled prior to production. Bell Aerosystems proposed a larger scale LFV, nicknamed the "Hopper" with an intended range of 80 kilometers each way. These projects and others were all given serious consideration, but abandoned as the Apollo program neared its end.[1] With the introduction of Constellation, it is time to reevaluate the feasibility and scientific potential provided by a lunar flying vehicle.

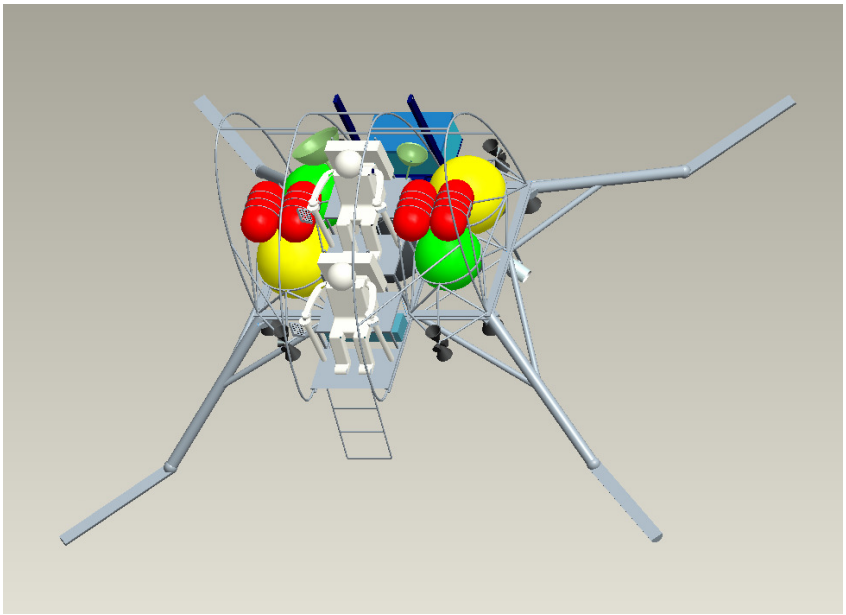

Figure 1. Alshain Model

Alshain is an LFV designed with the intent to seamlessly integrate with Constellation Architecture. The name Alshain is Arabic for falcon, and also a star located in the same constellation as Altair, the name of the lunar lander being designed for the Constellation program. Alshain makes several assumptions about the proposed Constellation architecture. Alshain utilizes cryogenic liquid oxygen (LOX) and liquid hydrogen (LH2) as its propellant source under the assumption that the Altair lander will be fueled by the same elements and will contain residual propellant that can be used to fuel Alshain. Constellation also seeks to explore the possibility of water ice pockets located on the lunar surface and to develop the infrastructure to extract and separate the water ice into hydrogen and oxygen to be used as propellants. Alshain assumes that when launched to the lunar surface, these in situ production facilities will already exist that the LFV can draw from. Finally it is assumed that the Lunar Relay Satellites (LRS) proposed by Constellation will be functioning to be used for communication and data exchange with the vehicle.

Mission Planning and Analysis

Egress from Altair Lander

Alshain is being transported to the moon on an Altair cargo mission. It is designed to be transported aboard the six-meter diameter cargo platform of Altair after the full construction of the lunar outpost (estimated 2020). Because the surface architecture will already be established, crews will be able to take advantage of the tools at base to unload Alshain from the cargo bay. These tools include the Tri-ATHLETE, the power supply unit (PSU), the lunar surface manipulator system (LSMS), and the Crew Mobility Chassis (CMC). The Three-legged All-Terrain Hex-Legged Extraterrestrial Explorer, Tri-ATHLETE, is a unit that can be operated either autonomously or with minimal crew involvement to unload payloads, up to 14.5 tons, from the cargo bay of the Altair vehicle. It either relies on its internal power supply, which is a 6.5 KWh Li-ion battery, or the PSU that enables a 5 km range. The Tri-ATHLETE comes fully equipped and stowed on each cargo mission to unload the payload bay as shown in Figure 2.[2] The LSMS allows the Alshain Lunar Flying Vehicle to be removed from the Tri-ATHELETE and placed wherever desired. It has the ability to lift up to 6 tons. Figure 3 shows the LSMS mounted to a CMC, which can tow up to 3,000 pounds and can operate either autonomously or manually.[3]

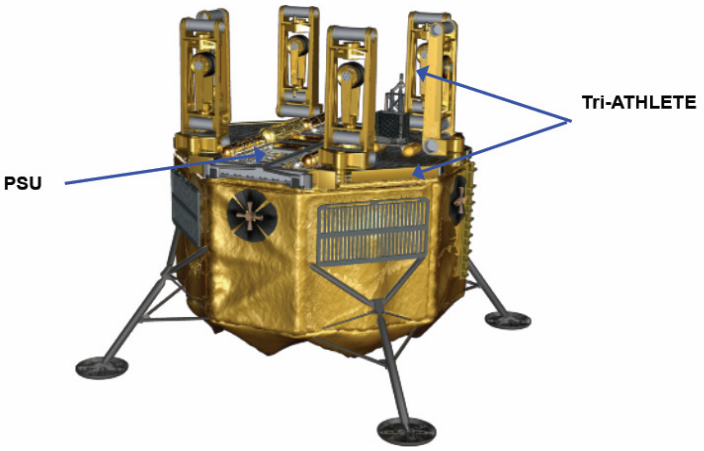

Figure 2. Image of the Altair lander with the Tri-ATHLETE and Power Supply Unit stowed on the cargo bay.

Figure 3. The Lunar Surface Manipulator System mounted to the top of a crew mobility chassis to maximize the range of unloading from Altair.

Mission Plan for Egress of Alshain

In order to unload Alshain from Altair several tasks have to be undertaken. The first task will be completed by the Tri-ATHLETE unit integrated with a PSU. The Tri-ATHLETE's back two legs will step onto the cargo bay of the vehicle to ensure clearance of Altair's component such as landing gear and RCS thrusters. The front four legs will roll along the lunar surface as the back two roll along the cargo bay. At the end of the bay the back to legs will step onto the lunar surface and the Tri-ATHLETE will move away from the base.

Once the Tri-ATHLETE has cleared the Lander, the Lunar Surface Manipulator System, mounted to the Crew Mobility Chassis, will connect to Alshain's roll cage and lift it off of the Tri-ATHLETE. It will then move

Alshain to the launch pad where the landing gear will be re-attached for flight. Reattaching the landing gear will require a crew EVA to fasten them into place. The LSMS and Tri-ATHLETE will then return to the lunar base.

Exploration Range

Once the LFV lands at an exploration site, the distance which astronauts are able to travel away from the vehicle dictates the design of mission plans. Exploration range is based on the safety of astronauts and thus restricts sites that they will be able to visit. The safety of astronauts is dictated by many different factors such as the occurrence of solar particle events and reach of lighting.

Solar Particle Event

In order to ensure safe travel back to base after a strong solar particle event (SPE), an analysis was completed of the amount of time it takes an astronaut to return to the safety of the lunar base site. Carrying shielding for an SPE aboard Alshain would require additional inert mass on the order of hundreds of kilograms, and thus the astronauts will be required to return to base during an SPE. Completing this analysis required knowledge of the anatomy of the astronauts and the limitation of their motion. The first analysis that was completed used Alexander's Formula.[4]

$$speed = \left(0.25\sqrt{g}\right)(stride^{1.67})(hip^{-1.17})$$

Where speed is the average foot speed, g is earth's gravitational constant, stride is the stride length, and hip is the hip height. For a 95th percentile American male, the hip height is equal to 0.882 meters and for a 5th percentile American female, the hip height is 0.825 meters.[5] In order to find the maximum walking speed on the moon, the relation for running was used.[6]

$$\frac{stride}{hip} \geq 2.9$$

The stride length for the male was equal to 2.56 meters and 2.39 meters for the female. As a result, the maximum foot speed for a 95th percentile male astronaut of 1.75 m/s and 1.71 m/s for a 5th percentile female. From these numbers, the exploration range as a function of time of flight was created, seen in Figure 4. This demonstrates the distance an astronaut can travel away from the base site if they are informed of the solar flare incident thirty minutes before the effect of the solar flares reaches the moon. This allots fifteen minutes for the crew to enter the vehicle at the exploration site and exit the vehicle at the base site. The remaining time, 15 minutes, is split into walking time and time of flight. As shown from this figure, the male and female results follow the same trend, however the female's walking velocity is the limiting factor. This plot can be used to determine the exploration distance an astronaut can achieve at any given range.

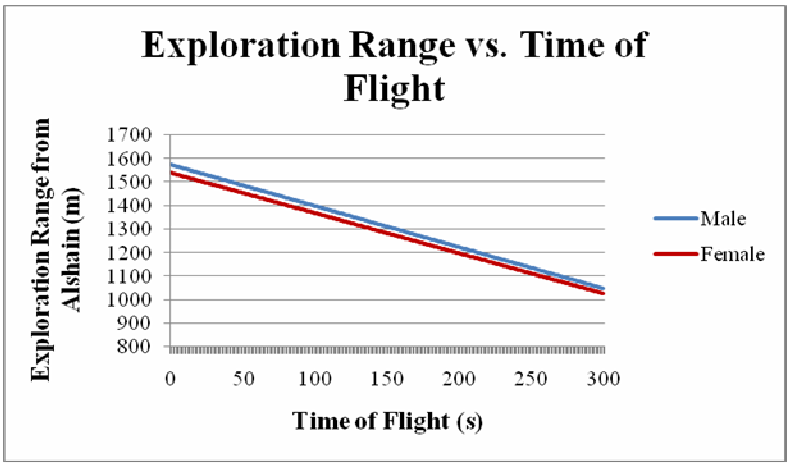

Figure 4. Exploration range of male and female astronauts as a function of time of flight.

Payload Bay Sizing

The Alshain payload bay has a contingency requirement to support an incapacitated astronaut in emergency situations. For the payload bay to be compatible with an upright-seated astronaut, the platform must support payload weights of 170 kilograms and payload platform area of 0.86x1.0m with a clearance height of 1.49m (volume of $1.28m^3$).

Using these payload bay parameters as a baseline, it was essential to analyze whether these parameters would allow the Alshain payload bay to be adequately compatible with common scientific payloads. Thus, a database of 104 payloads was constructed from NASA documents consisting of past Apollo science payloads and future science payloads slated for use on the Moon and Mars. The study analyzed how many of the individual payloads would be compatible with the payload bay for a given mass or a given volumetric limit. The aim was to conclude whether mass and volumetric limits of a standard mission payload dictated the cargo bay, or if in fact the size of a downed astronaut was sufficient size for the payload bay. By analyzing scientific paylods, the point of diminishing returns would dictate a 40kg payload bay capability. This is well within the range of the requirements of supporting a downed astronaut. The same can be seen with the volume of the payload bay versus percentage of compatible payloads. Point of diminishing returns would dictate a $.28m^3$ meter payload bay volume, well within the range of the requirements of supporting a downed astronaut.

Locking Mechanism for Payload Bay

In order to safely secure payloads, an adaptive method was created which allowed for payloads of different shapes and sizes to be stowed and removed by astronauts while on EVA. The payload bay platform will be made out of an aluminum isogrid. The isogrid will contain a series of equilateral triangles where mushroom locking mechanisms will fit to secure the payloads. Payloads will not only be placed in a predetermined location to balance the payload bay center of gravity, but their fixed location will prevent shifts in the C.G.

The isogrid material has a high strength to weight ratio. The largest payload is that of a downed astronaut. For this scenario, a payload bay attachment is fitted into the isogrid floor. The attachment contains a seating area equipped with a PLSS locking attachment and foot constraints to keep the astronaut within the 0.86x1.0m platform area and a clearance of 1.44 m for a 95^{th} percentile United States male. The isogrid has been designed to support the 170kg payload mass of the downed astronaut.

Craters

Craters are important locations to visit for both scientific and logistical reasons. Since craters are formed by impacts from extra lunar bodies, such as meteorites and comets, the crater floors often contain deposits of materials that would not be normally found in the regolith on the surface of the moon. Of particular interest are deposits of hydrogen, which have been detected in the bottoms of certain craters and may indicate the presence of water. Older and larger craters tend to gather larger amounts of volatiles, as they contain smaller craters within them.

Additionally, crater floors that are protected from exposure to direct sunlight, due to crater depth and location, will contain larger quantities of intact volatile compounds than otherwise. These include water molecules, which would evaporate and be lost if exposed to sunlight. The craters near the lunar base site, because of their proximity to the lunar south pole, remain in nearly perpetual darkness.

The considerations for the selection of potential mission sites for the Alshain vehicle include the distance from the base site on the rim of a particular crater, crater depth, and potential significance regarding both scientific studies, and potential for in situ propellant mining, which relies on the presence of hydrogen or water.

Reference Mission

The Alshain Lunar Flying Vehicle will provide transportation for astronauts to sites of interest that are inaccessible by rover. One of Alshain's potential missions includes a trip to the Shackleton Crater Basin (89.9º S, 0.0º E) because of the possible presence of hydrogen and water, as well as its proximity to the lunar base site. Shackleton Crater is 19 kilometers in diameter and 2 kilometers deep. Alshain will transport astronauts a total of 20 kilometers (10 km to a mission site and 10 km back to base) with a total time of flight of just 3.7 minutes (3 minutes, 42 seconds).

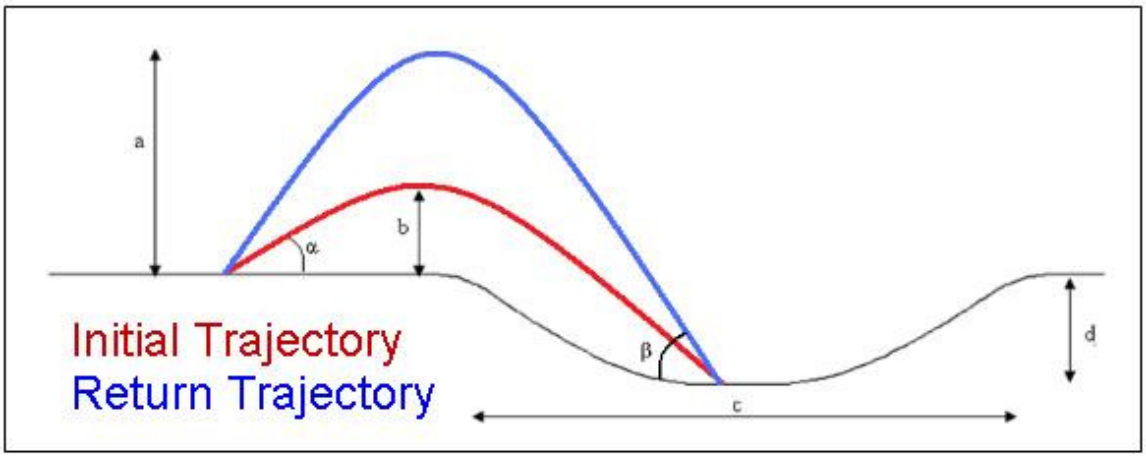

a (km)	b (km)	c (km)	d (km)	α (°)	β (°)
3.6	1.6	19	2	38.7	50.2

Figure 5. Ballistic Hop Trajectories for Mission to Shackleton Crater

The Tsiolkovsky rocket equation was used in order to calculate the change in velocity (ΔV) necessary to attain the flight trajectories shown in the reference mission.

$$\Delta V = V_e \ln\left(\frac{m_{final}}{m_{initial}}\right)$$

Where V_e is the exhaust velocity of the rocket engine, $m_{initial}$ is the initial mass of the vehicle, and m_{final} is the mass post-burn.

The ΔV calculations for the reference mission were based on equations developed for ballistic hops and glides on flat, airless bodies. A flat, airless body is a good approximation because the moon has no atmosphere and the distance traveled is small compared to the moon's radius. For the reference mission, the total amount of ΔV necessary was calculated by splitting the mission into three stages. The first stage is a ballistic hop 10 km horizontally and -2 km vertically into Shackleton Crater. The second stage is a 3 km flat glide along the bottom of the crater, which accounts for locating a suitable landing area. Finally, the third stage is a hop 10 km horizontally and 2 km vertically back to the base site.

The total ΔV required for the reference mission to Shackleton Crater is approximately 710 m/sec. The first and third (ballistic hop) stages each require 250 m/sec and the second (propulsive glide) stage requires 197 m/sec.

Refueling

Plans for refueling the Alshain assume that in situ propellants on the moon are made accessible by a propellant processing station provided by the Constellation Lunar Surface Architecture. This station will have both the capability of processing residual propellants from the Altair Lunar Lander as well as the in situ propellants on or within the lunar surface and all the necessary equipment to transport cryogenic propellants to and re-supply Alshain.

Return to Base

A 10m x 10m landing pad will be used to enable the Alshain to land as close as possible to a lunar base while preventing hazardous ejecta upon landing. After considering different materials for the landing surface, the use of a fire blanket (commonly used by firefighters) was found to be a simple yet viable solution. The Insulflex Pyroblanket (17oz) has the ability to remain intact under temperatures up to 1500 K and is made of silicone rubber that has a mass of 60 kilograms for a 100 square meter area.

Dust Maintenance

During the Apollo missions, it was found that accumulation of moon dust on astronauts, tools, and vehicles can pose a serious problem. During these missions, it was found that lunar dust clings to astronauts and equipment and is very abrasive. The assumption was made that Project Constellation architecture will include a dust mitigation

strategy that will be applicable to the Alshain. One dust mitigation concept that is being investigated is an "electric curtain" composed of parallel electrodes that will sweep such particles off its surface.[7]

It will be necessary to periodically remove dust from important components and mechanisms of the Alshain between missions. Key areas include control panels, the main engine nozzle, reaction control system nozzles, PLSS connectors, and the payload elevator.

Loads, Structures Mechanisms

Loads

Table 1. Loads Table

Event in Lifecycle	Type of Load	Load
Launch	-Z	6g
Launch	+/- X, +/-Y	2g
Launch	+Z	2g
Launch-Steady State	+/- X, +/- Y, +/- Z	1.9g --- 1.25g
Landing	-Z	2g
Flight-Main Engine	+Z	2g
RCS Thrusting Vertical	+/-Z	1150 N
RCS Thrusting Horizontal	+/- X, +/-Y	300 N
Kick Loading	+/- X, +/- Y, +/- Z	250 N
Rollover Loading	-Z	1.64 m/s²

CG Analysis

The following equation was used to calculate the center of gravity (CG) location for pre-flight and post-flight Alshain configurations:

$$\vec{cg} = \frac{\sum mass * \vec{x}}{\sum mass}$$

The CG location was measured relative to a point along the engine's axis of symmetry, 0.1 meters from the bottom of the engine bell. For pre-flight configurations, mass and relative location of each individual component of the craft is taken into consideration. For post-flight configurations, expendable items on the vehicle (such as propellant), will either be depleted or offloaded at the mission site. The two CG locations of the pre-flight post-flight configurations bound the envelope within which the center of gravity shifts during flight.

Another CG-shift consideration is the range of crewmember masses. The "nominal" configuration of Alshain assumes the largest possible astronauts as the main crew (170 kg each).

Table 2. Nominal CG Location for Alshain

	Pre-Flight X (m)	Pre-Flight Y (m)	Pre-Flight Z (m)	Post-Flight X (m)	Post-Flight Y (m)	Post-Flight Z (m)
Nominal Configuration	0.015	3.48E-04	0.437	0.017	5.63E-04	0.368

The CG was analyzed using 18 different test cases. Each case investigates a different mass distribution including alternating masses of crew, differing payload sizes, and unmanned operations. The extreme cases of CG shift were used to determine the maximum CG shift envelope.

Table 3. Max CG Shift per dimension

	Shift (m)	Case
Max X-CG Shift (m)	0.164	Crew: One 95th percentile male; no cargo
Max Y-CG Shift (m)	8.79E-04	Crew: None; no cargo
Max Z-CG Shift (m)	0.452	Crew: Two 95th percentile males; no cargo

Support Structure Rationale

As seen in the loads table, the main causes of loading are axial (z-axis), especially in the cases of functioning on the moon. The configuration of the components of the main vehicle is relatively short axially (1.46 m in the z axis), while being relatively wide and deep (y and x directions respectively).This causes large moments to be created by the primarily axial forces, while not allowing for a tall structure to distribute the loading.

In order to counter these large moments, a single support base in the x-y plane and a truss structure were considered. Due to spacing issues with the rocket and crew, a truss system would be impractical. This leads to the use of a single support structure rather than a truss structure.

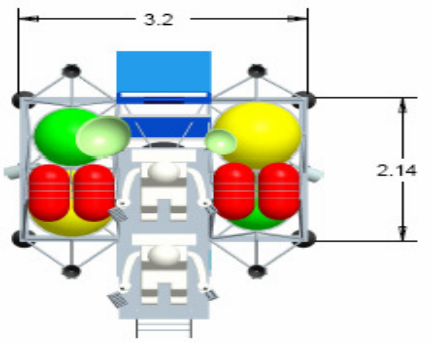

Figure 6. Alshain Support Structure Top View

Support Structure Placement and Shape

The two options considered for placement of the support structure were around the middle of the fuel tanks, and flush with the bottom of the fuel tanks.

Bottom	Middle
• Open space away from other components • Lower attachment for landing gear • Rests on support structure when stowed • Struts required to transfer loads to support structure	• Blocks crew access • No struts required to transfer loading to support structure • Support structure required to fit between other components

The benefits of the lower attachment point were determined to outweigh that of the middle attachment point. The shape of the support structure is determined by the x-y plane configuration of the vehicle. The two sets of tanks and engine/crew area form three distinct sections, which are outlined by the support structure. This allows for support struts to be placed around the outside of each essential structure and have each main component supported in each direction.

Beam Choice

The choices for beams used in the support structure are determined by an analysis of internal moments and shear forces, with torsion as a secondary concern. Hollow tubular beams and I-beams have been selected for their strengths in taking these three types of forces. The analysis of moment and shear forces concluded that a support structure made of the I-beams would be 40kg less massive than a set of hollow tubular beams. This leads to the choice of I-beams with a 40kg envelope to prevent torsion effects.

I-Beam Analysis

The analysis for I-beams is done by setting the total height and width of the I-beam cross-section and solving for the necessary flange and web thicknesses with a minimum set at 2mm. The web thickness is calculated for failures in shear and vertical Euler buckling.

$$\sigma = \frac{F}{Height * t_{web}}, F = \frac{\pi EI}{(KL)^2}, I = \frac{t_{web} Height^3}{12},$$ K = 0.5: fixed-fixed

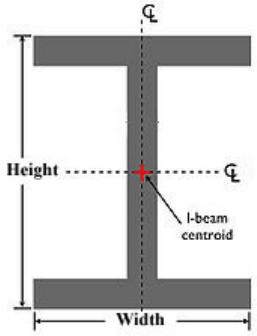

Figure 7. I-beam analysis

The flange thickness is then calculated for bending forces.

$$\sigma_{yield} = \frac{Moment * Height}{2I}, \quad I = \frac{WH^3 - H^3 Wt_{web}}{12}$$

The height of the I-beam is determined by mass, clearance for the rocket nozzle, height in stowed configuration, and machinability. I-beams of 10cm height would be flush with the bottom of the rocket nozzle, while anything larger would increase the stowed height of the vehicle linearly. The results of the trade study show that mass savings significantly drop after 12.5cm height due to the 2mm thickness requirement. This allows for 2.5cm clearance for the rocket nozzle while stowed and is at the point of diminishing returns for mass savings.

Component Attachment System

Due to the choice of support structure placement, an array of small pinned struts is necessary to join each specific component to the support structure. To handle the primarily axial, hollow tubes have been chosen throughout the structure as the truss members. This member choice leads to the analysis of each truss member for solely tensile and compressive forces.

Tubular Member: Axial Loading Analysis

Each tubular member has been considered for four failure types: Tensile strength, compressive strength, Euler buckling, and tubular "shell" buckling.

Tensile failure and Compressive: $\sigma_{yield} = \frac{F}{A}$

Euler buckling: $F = \frac{\pi^2 EI}{KL^2}$, $I = \frac{\pi}{4}(R^4 - (R-T)^4)$, K=1

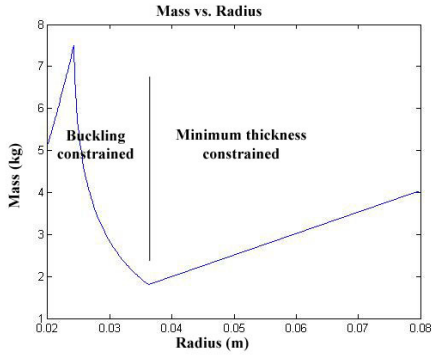

Figure 8. Mass vs. Radius

Tubular "shell" buckling: $\sigma_{yield} = \frac{TE}{r(1-v^2)^{1/2}}$

*-In practice slight machining of 15% wall thickness cause shell buckling failures to occur at 50% of ideal stress values, so the yield stress was doubled for all calculations.

These formulae have been applied to each strut design and the thickness for each beam has been determined for a given radius using a minimum of 2mm for machinability. Tubes are chosen to minimize mass within a reasonable radius for spacing considerations.

Support Structure Crossbeams

Support structure crossbeams are necessary to maintain stability. The inner area has a natural protection against collapse from the rocket engine, but the outer sections require additional support. Because the I-Beams are secured in a stowed configuration, the worst case loading scenario for collapse of the support structure is 2m/s^2 lateral force during a two leg landing, corresponding to a shear force of 4,000 N. This distributes to the symmetric crossbeams, leading to a compressive force of 3960 N. Running a tube analysis for compression over a range of radii leads to an ideal beam size of 1.6cm radius, 2mm thickness and 0.8kg mass per member.

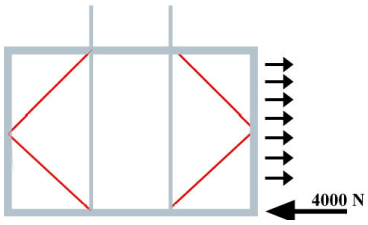

Figure 9. Support Structure Loading

Fuel Tank Support Structure

The fuel support structure is designed to connect the LOX and LH2 tanks to support structure below. The stowed (without fuel) load scenario and take-off and landing scenarios (with fuel) were considered. Under the worst case scenario the LOX tank creates an axial force of 7630 N and a lateral force of 763 N, while the LH2 tank creates a 1270 N axial force and a 127 N lateral force.

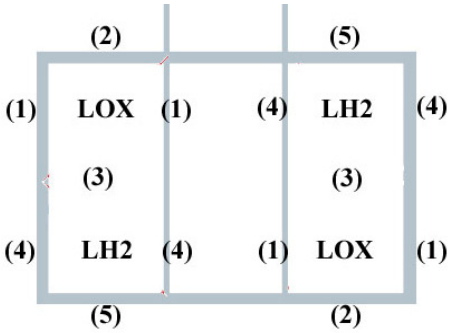

Figure 10. Fuel Tank Support Structure

Each numbered point in Figure 10 refers to a pair of supports placed at a 45 degree This translates into compressive force within the beam by using the following equation.

$$F_{compression} = \frac{(F_{axial} + F_{lateral})}{2\cos(45)}$$

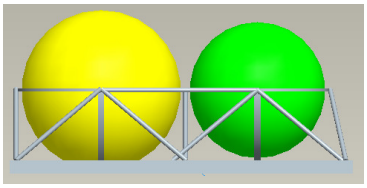

Figure 11. Fuel Tank Support Structure Side View

Rocket Support Truss

The rocket support truss serves a dual purpose in that it supports the rocket, but also braces the central support structure against collapsing forces, with attachment points at corners to minimize torsion. The 6G axial stowed and 2G lateral loads (compressive) and the take-off case of 40kN (tensile) are the worst cases. The beams are oriented at θ=53.3 from the z axis. The tension and compression forces are

$$F_{tensile} = \frac{F_{rocket}}{4\sin(\theta)}, \; F_{compression} = \frac{F_{axial}}{4\sin(\theta)} + \frac{F_{lateral}}{2\cos(\theta)}$$

This leads to an applied tensile force of 12.5 kN and a compressive force of 3.757 kN. The tubular member analysis concluded that the determining failure was due to the compressive force.

Table 4. Margin of Safety

Tube Inventory	**Piece Designation**	**Applied Load (N)**	**Breaking Load (N)**	**MOS %**
Engine Support	**Engine Support Tube**	12,500 (Tension)	improbable failure case	1000+
		3,757 (Compression)	13,100	25
Fuel	**LOX Support**	1,484 (C)	2,368	14
	LH2 Support	248 (C)	424	22
	Middle Support	1,731 (C)	2,690	11
Crew	**Vertical Support**	1,000 (C)	1,435	2.5
Main	**I-beam Crossbar**	3960 (C)	5,821	5
I-beam	**Piece Designation**	**Applied Force**	**Breaking Force**	**MOS %**
Lengthwise	**Shear Force (N)**	12,500	50,000	
	Moment Force (N-m)	4,125	5795	0.35
Widthwise	**Shear Force (N)**	3,000	50,000	
	Moment Force (N-m)	3,300	4,948	7.10
Crew Support	**Shear Force (N)**	4,670	50,000	
	Moment Force (N-m)	3,180	4,948	11.14

Fuel Tank Cradles

In order to secure the LOX and LH2 tanks within the structure, semicircular cradles with rectangular cross sections are used. A cradle cross section thickness (measured radially from tank center) was chosen and the cross section width (completing the rectangular cross section) of the various cradles was varied. The analysis was completed using Pro-Engineer FEA due to the complicated nature of the loading and structure. The LOX cradles are 2.6kg each and the LH2 cradles are 0.6kg each.

Crew Platform

For the crew platform, a honeycomb will be used to support astronauts. The worst case loading of 2 g's was used, which corresponds to 3400N from the astronauts. Aluminum Flex-Core honeycomb was chosen. The specific designation is CR-PAA-5052/F40-.0013"-2.1", which has a phosphoric acid anodized coating, 5052 aluminum alloy and has density of 2.1lb/ft^3. Each honeycomb cell will have dimensions of .75" width, .75" length, height of .25", and an individual wall thickness of .0013". With this dimension, this honeycomb can stand up to 1.4GPa. The total mass of crew platform is 1.44 lb, which yields 0.66kg.

Roll Cage

The roll cage is designed to shield Alshain's crew and sensitive components from rollover. It is dimensioned to provide a 30-centimeter clearance at all points around the crew and pressure tanks in order to protect from obstacles 30 centimeters or less in height. The design includes 4 elliptical arches, each 2.4m tall, connected by a total of 7 crossbars (3 on each side of the tank compartment, 1 bracing between the crew compartment). The roll cage can withstand up to $6g_{moon}$ forces with a safety factor of two. The maximum specifications of the roll cage are listed below.

Table 5. Roll Cage Margin of Safety

Member	Bending Stress (MPa)	Compressive Stress (MPa)	Margin of Safety	Mass (kg)
Crew Cage	1.04E-03	24.8	5.28	12.26
Tank Cage	4.14E-03	68.9	1.25	3.92
Tank-Crew Crossbar	N/A	60.4	1.56	0.85
Crew-Crew Crossbar	N/A	60.4	1.56	0.89

Landing Gear

Being able to absorb landing shock is critical to mission success. In the case of Alshain, the vehicle must be able to absorb a 3 m/s vertical velocity and a 1 m/s horizontal velocity while landing on a 15 degree slope and negotiating a 30 cm high obstacle. The Altair lander uses crushable honeycomb for its deceleration media, but it is only a one time use material. The Alshain must be able to land repeatedly so springs are required.

The first criteria to determine is how many legs the Alshain should have. Given that in a worst case load landing scenario the craft will land on one leg, for a given vehicle mass, all the legs must be the same mass and size regardless of the number of legs. A further consideration is the tipping protection provided by the leg arrangement. In a worst case tipping landing scenario the vehicle will land across two adjacent legs. In this situation the center of gravity of the Altair can only provide counter torque with an effective moment arm of the projected leg length in the tipping direction. This can be seen in Fig. 1 below.

Since the legs are all the same size for a given vehicle mass, the tipping protection per unit mass of legs is given as the effective moment arm for a given leg length, r2/r1, over the number of legs. Analyzing the picture above yields four legs as the most mass effective solution.

With the number of legs established the leg dimensions must be found. The dimensions are constrained by the crew acceleration limit of two Earth g's. Solving for an appropriate single spring that is aligned at the proper angle to cope with the respective landing velocities shows a horizontal acceleration that is too high to be handled without tipping. Thus two separate springs must be used to handle the vertical and horizontal accelerations separately. Optimizing for minimum leg mass gives a leg that is 2.3 meters from the base to the tip, has a vertical stroke of .82 meters (using torsion springs), an uncompressed height of 1.33 meters, and a horizontal spring contained in a separate footpad at the end of the leg that is 1.64 meters long in stroke to prevent tipping by using a low acceleration as seen in Fig. 2 below.

After analyzing the worst case loading set up and allowing for a machinable thickness of no less than 2 mm it was determined that the constraining loads would be bending and Euler in nature. This presents an optimal leg design of a round tapered hollow beam that eventually becomes a cylinder out at the end. The final mass of the leg assembly is roughly 22 kg per leg, or 88 kg overall mass (including lateral supports to help with distributing loads to the frame).

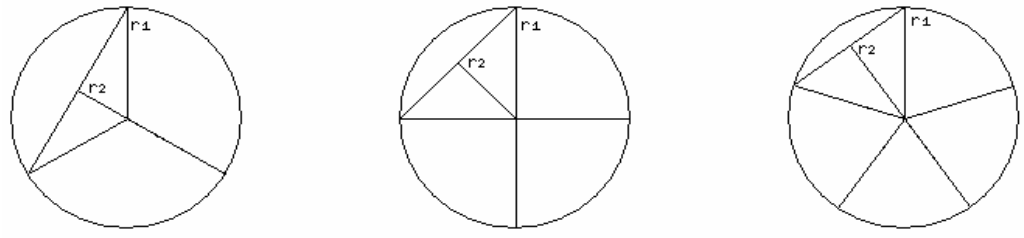

Figure 12. Landing Gear Analysis

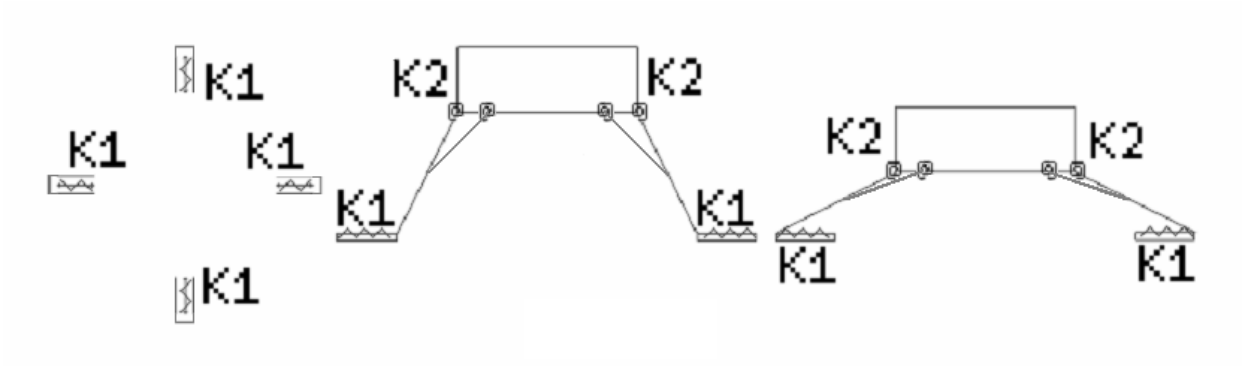

Figure 13. Landing Gear Spring Configuration

Cold Rated Spring

For the landing gear a torsional spring will be used. The requirement for choosing the spring material is that it must function in lowest temperature in the moon, which is 80K, without fracturing in a brittle manner. It also needs to be a face-centered cubic crystal material to avoid ductile-brittle transformation. The material chosen for this requirement is copper-beryllium. This material does not undergo any low temperature allotropic phase transformations and works well at low temperatures. This material can also stand up ~1300 K. For the consideration of landing loads, this material has a tensile strength of 240-280 MPA, and modulus of elasticity of 125-130 GPA.

Thermal Shield

To shield the landing gear from the engine plume, the landing gear will be covered with thermal shielding. The chosen thermal shield is a Flexible Insulation Blanket (FIB). The FIB has low density and has the ability to withstand high temperatures. This thermal shield can stand up to 1700K, is made out of ceramic matrix composite, and is easily machinable. When covering the landing gear legs with this thermal shield only half of it will be covered because the engine plume will only contact the inner half of the leg. The dimensions and the mass of FIB are calculated below:

Table 6. Landing Gear Thermal Shield

Number of Legs	Radius (m)	Length (m)	Thickness (m)	Area (m^2)	Mass (kg)	Total Mass (kg)
4	0.065	2.9	2.54E-04	0.59	0.022	0.087

Crew Systems

Contingency Radiation Protection

Contingency radiation protection was found to be unnecessary based on a 0.05% probability of a dangerous Solar Particle Event (SPE) occurring in a 24 hour period and a mission reliability of 99.2% (See Appendix C). With a project lifetime of 250 missions, the likelihood of both a mission failure and dangerous SPE event occurring simultaneously is less than 1 in 1000.[8]

Crew

Design considerations included accommodations for crew members ranging from 5th percentile American females through 95th percentile American males. The range of suited crewmember masses considered was 120 kg – 170 kg. The range of suited crewmember heights considered was 1.7 m – 1.9 m.[9]

Seating

The seating configuration was based on rover seats which are designed to accommodate EVA suited astronauts.

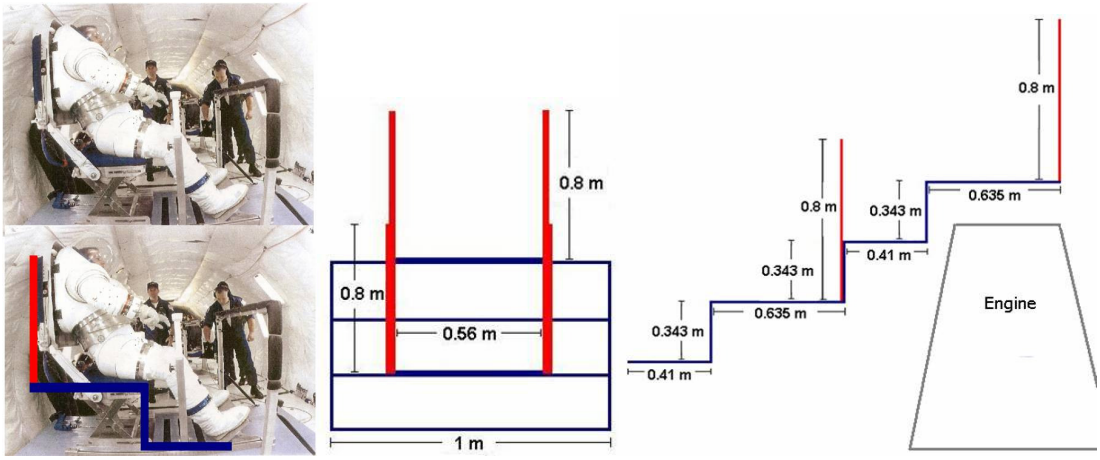

Figure 14. Crew Seating

Seat dimensions were based on the results of a partial gravity rover seating design study. [10]

Restraints

The red bars shown in the previous figures represent Personal Life Support System (PLSS) supports and restraints. By restraining the PLSS, the hard upper torso of the Constellation spacesuit is also restrained from motion. The crew's feet are restrained from kicking up during flight by boot restraints located at the back of the heel.

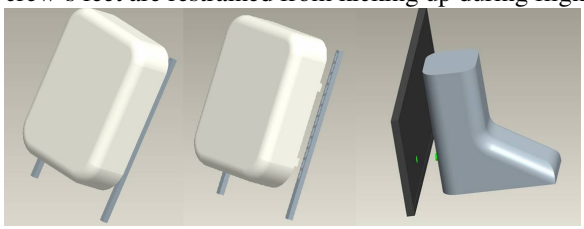

Figure 15. PLSS and Boot Restraints

Sightlines

The nominal pilot of the Alshain is the forward crewmember. The limiting factor of the sightlines of the forward crewmember is their own lower body (limited to 45° downward). The aft crewmember is also supplied with a set of control towers and is able to pilot the craft in a contingency situation. However, the sightlines of the aft crewmember are further obstructed by the forward crewmember (limited to 30° downward).

Hardware Testing

Hardware testing was conducted to confirm the feasibility of ingress/egress as well as an incapacitated astronaut rescue. Suited ingress and egress was successful, aided by handholds provided by the roll-cage structure. Incapacitated astronaut rescue testing is ongoing. Hardware testing images are attached in Appendix E.

Elevator

The hardware elevator consists of a 1 by 0.6 m wooden elevator platform attached to two 1.7 m aluminum guide tracks. The elevator platform is raised and lowered using a high torque AC motor which winds a lifting rope.

The main advantage of an elevator is its small footprint. With an elevator, the elevator platform acts as the vehicles payload bay. Once the payload is loaded onto the elevator, the platform is raised to its flight position and the payload remains there. With a winch, there needs to be room for the payload, room for the winch to be mounted

Figure 16. Hardware Payload Elevator

and swing, and room for an astronaut to stand and operate the winch. This results in a 90% larger footprint for a winch system. This means a larger, more complicated, and heavier vehicle structure.

The elevator also has the advantage of being a symmetrical system. When the elevator is mounted on the rear of the vehicle it maintains its lateral symmetry, simplifying the center of gravity calculations and minimizing use of the reaction control system.

Chosen Design

After hardware testing was completed, the elevator was chosen as the payload loading system. The elevator was chosen due to its smaller footprint and symmetry. The smaller elevator footprint allows Alshain's stowed area to be nearly 10% smaller than it would be with a winch. This makes the vehicle easier to send to the moon as well as load and unload from the Altair. The elevator was redesigned based on knowledge gained from hardware testing.

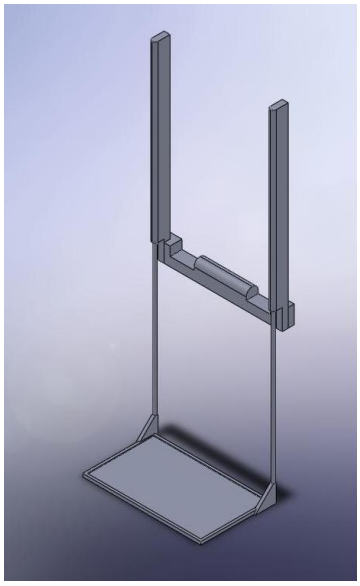

Figure 17. Payload Elevator Model

Lighting

The lighting configuration on the lunar flying vehicle must ensure sufficient illumination to allow safe flight in daylight and night conditions. In all crew control areas, the lighting must be able to dim in order to accommodate different contrast conditions. The lighting must also be able to properly function in the unpressurized, temperature-varying lunar environment. For this reason, halogen lamps were chosen over LED lamps, as LED lamps would require an extra pressurized housing in order to operate in lunar conditions.

Table 7. Summary of Lighting Configuration

Group	**Purpose**	**Location**	**Type / Model**	**Qty**	**Power (W)**	**Mass (kg)**
Vehicle	Illumination of crew flight control area, contingency lights	Above aft crewmember, on roll cage bars	Halogen flood lamps	2	40	1
Vehicle	Illumination of crew ingress / egress area	Below fore crewmember, directed at ladder	Halogen flood lamps	1	20	0.5
Vehicle	Illumination of cargo area	On roll cage cross bar above cargo area	Halogen flood lamps	1	20	0.5
Surround	Illumination of landing gear legs and vehicle vicinity	On each corner of main platform, each pointed at one leg	Halogen flood lamps	4	200	3
Surround	Illumination of potential landings sights	One on either side of the main platform	Polarion PF40 searchlights	2	80	16
Mission	Illumination of miscellaneous task areas	Helmet-mounted or shoulder-mounted	Constellation Space Suit System (CSSS)	2	--	--
Mission	Portable Illumination of mission task areas	Stowed for portable use	Fluorescent / Incandescent combination lamps			

Debris protection

The engine plume of the Alshain has enough energy to eject lunar particles around the vehicle during takeoff and landing to high speeds. These particles have potential of redirecting back towards the Alshain. Because the Alshain is not a pressurized vehicle, it is open to the lunar environment, and high-speed lunar ejecta poses a threat to the crew on board. Proper debris protection is required for this reason. To save mass and space on the vehicle, a non-structural debris shield configuration was chosen. The body of a crewmember will be protected by an extra Thermal and Micrometeoroid Garment (TMG) debris shield, worn like a sleeved blanket and clipped to the metal ring that connects the space suit helmet and Hard Upper Torso (HUT). The head of a crewmember will be protected by a polycarbonate shield that snaps to the top of the PLSS and clips to the metal ring that connects the space suit helmet to the HUT. Both of these shields will be put on before takeoff and removed after landing, so as to not hinder operations outside of flight.

Table 8. Summary of Debris Protection Design

Group	**Purpose**	**Materials**	**Total Mass per Crewmember (kg)**
TMG debris shield	Protect the body of the crewmember from high-speed lunar ejecta particles	Ortho-fabric Gore-Tex®/Nomex/Kevlar Low Density Linear Polyethylene (LLPE) Neoprene Coated Nylon Ripstop	4.6
Head debris shield	Protect the head of the crewmember from high-speed lunar ejecta particles	Polycarbonate	7.8

Avionics

Avionics Overview and C&DH

Alshain's avionics system controls most of the onboard vehicle's systems. Its functions include automatic determination of the vehicle's status, operational readiness; performance monitoring; digital data processing; communications; guidance, navigation, and control.

Avionic systems are designed to withstand multiple failures through redundant hardware and software. These are managed by a complex of four computers to meet the two-fault tolerance level one requirement. After one failure in the system, redundancy management allows the vehicle to continue on its mission. After a second failure, the vehicle still is capable of returning to a landing site safely.

In aid to Alshain's avionics, we will be using Lunar Relay Satellites (LRS) as part of the Constellation program. These LRS will be put in lunar orbit for the purpose of guidance, navigation and communications. LRS' will be in 12 hour orbits around the moon with eight hours exposure over the South Pole region. These satellites are capable of one-and-two way ranging and are fully capable of relaying both S and Ka band communications. They also have the capacity to store and forward data with 300 GB.

These satellites will serve the same purpose that TDRS serves for near earth network communications. These satellites will primarily be used for command and telemetry between the vehicle and the lunar base. However if Alshain is at a location where it can not make direct to earth communications link to the Deep Space Network (DSN) antennas on Earth, LRS' will be used as a medium to create the link.

Alshain is required to communicate directly to the lunar base. Lunar Communications Terminals will be mainly used to server this purpose. These terminals will be planted very close to the lunar base and are capable of transmitting both S and Ka band along with both 802.16e and 802.11. They are capable or one way ranging for emergency return back to the base.

The Command and Data Handling (C&DH) system behaves as the LFV's brain. It distributes commands, records telemetry, and keeps various components' status updated in real-time. The C&DH is comprised of an enclosure, a backplane, four single board computers, S-band and Ka-band communications interface boards, data storage boards, a housekeeping and digital input/output board, and analog data acquisition boards. All electrical connections between these components are made via the backplane for internal power distribution and PCI bus data transfers. The interfaces between the C&DH and other avionics components are connected through a SpaceWire

network. Network provides for a standard that enables high and low data rate communication between avionics components over the vehicle. This network highly increases speed and reliability in space-flight systems.

Guidance

The vehicle will follow a modified ballistic trajectory, transitioning into a propulsive glide on the final approach to the destination to allow the crew to visually inspect the landing site and redesignate the target as necessary. Control levels are provided for three different levels of human involvement—autonomous, direct, and teleoperation. Under autonomous control, the vehicle's onboard computers will manage all aspects of flight without the need for external intervention. The destination will be specified prior to launch and a lidar scan will be conducted to identify a safe touchdown location free of hazards. Under direct control, automatic control loops will maintain pilot-specified rates, both in translation and rotation. Teleoperation is similar to the autonomous mode, with the exception that the lidar scan will be transmitted to a remotely located pilot and human judgment will be used to select the landing site.

Navigation

In the absence of a hard navigational requirement, 100 meters was selected as the maximum acceptable three-sigma navigational error to ensure the vehicle will end up within line of sight of the desired target. Once a position and attitude fix is determined from external references prior to launch, the vehicle will be capable of reaching the destination under inertial navigation alone (with the exception that ranging to the ground may be necessary at the very end to properly null velocities for landing). The system was designed as such because it is not currently known whether navigational updates will be reliably available in flight.

There are very few ways to quickly determine one's position relative to an unseen reference (e.g., the origin of the Earth-Centered Inertial frame). It is for this reason that the GPS system was established on Earth; and NASA intends to set up a system of lunar relay satellites to serve this purpose on the moon. The achievable accuracy of position estimation using LRS ranging and terrain contour matching is approximately 10 meters, given several minutes for the solution to settle.[11] Of the options which exist for determining an initial attitude fix, star trackers were chosen because the stars are available as a reference from any location on the surface of the moon—as opposed to the sun or the earth which will not necessarily be visible. Star trackers are capable of providing full attitude information about yaw, pitch, and roll. Two units will be mounted pointing up from the top of the vehicle at an angle of 45 degrees, and separated by 90 degrees. This will enable attitude determination regardless of the sun vector. If neither unit is sun-blinded, then it will also eliminate the roll-axis uncertainty inherent to star trackers.[12] To help mitigate obstruction of the optical elements due to dust accumulation, covers will be placed over the baffles when not in use.

Error Budget

An estimate was made of the total expected final error in touchdown site due to the various sources of navigational error, both in the initial fix and in the inertial propagation of that fix. For the star trackers and inertial measurement units (IMU), reference units were selected which should be comparable to the devices used on the actual vehicle, namely the Galileo Avionica A-STR Autonomous Star Tracker and Honeywell HG9900 IMU. A redundant system of four such inertial measurement units will ensure that pure inertial navigation is possible even in the event of two IMU failures. The following table shows the estimated error characteristics of these references units, grouped into low and high frequency phenomena.

Table 9. Navigational Uncertainties

Uncertainty Source	Value	Units
Low frequency:		
star tracker bias	10	arcsec
star tracker low freq error	7	arcsec
star tracker noise	9	arcsec
LRS ranging	10	meters
accelerometer bias	75	μg
accelerometer scale factor	300	ppm
gyro bias	0.009	deg/hr
gyro scale factor	15	ppm
High frequency:		
angular random walk	0.006	deg / rt-hr

The contributions of each error source to the final position knowledge were combined to produce an overall estimate. A very conservative approach would be to directly add the error from each of these sources under the assumption that they all generate a worst possible error in the same direction. A less conservative approach would be to combine the errors in a root-sum-square under the assumption that they all vary independently. For the purposes of this analysis, a middle ground was chosen and the low and high frequency uncertainty sources were treated separately, with sums taken for each category which were combined in a root-sum-square. The equations used to propagate these errors are provided in Appendix F. The following table shows the final results for two reference missions. At maximum range, this system is capable of providing 38 meters accuracy, well within the desired vehicle performance.

Table 10. Error Budget

Uncertainty Source	**Shackleton Mission 10 km 173 secs, ā =1.95 m/s2 $\bar{v}$=74.7 m/s $\bar{\omega}$=0.01 deg/s**		**Shoemaker Mission 57 km 342 secs ā =2.08 m/s2 $\bar{v}$=202 m/s $\bar{\omega}$=0.007 deg/s**	
star tracker bias	0.5		2.8	
star tracker low freq	0.003		0.008	
star tracker noise	0.4		2.5	
LRS ranging	10		10	
accelerometer bias	1.1		4.4	
accelerometer scale	8.8		36	
gyro bias	0.05		0.5	
gyro scale factor	0.004		0.02	
	Subtotal (RSS):	**8.9**	**Subtotal (RSS):**	**367**
angular random walk	0.2		1.5	
	Subtotal:	**0.2**	**Subtotal:**	**1.5**
	Total*:	**9.1 m**	**Total*:**	**38 m**

*Totals include device internal errors only

Control

The initial launch and acceleration phases of the flight will follow pre-programmed guidance which specifies acceleration, velocity, attitude and attitude rates as a function of time. Once the acceleration phase is complete, control will change to a target-centric algorithm using a propagated trajectory based on the navigation data. The target during this phase is a point in space (with some tolerance) at which the deceleration phase begins. During deceleration, the radar altimeter will be incorporated and the thrust vector will be set so that the vehicle will have zero vertical velocity and a predetermined in-track velocity at some predetermined altitude. Thus, the vehicle will come out of the ballistic trajectory and into a propulsive glide at a specified altitude.

Thrust vectoring during the acceleration and deceleration phases is accomplished by altering the vehicle's attitude with the reaction control thrusters. Thrust vectoring during the coasting phase is accomplished using the reaction control thrusters themselves.

Status Monitoring

The vehicle shall monitor all critical parameters to enable identification and handling of faults. The two primary vehicle systems requiring status monitoring are the power and propulsion systems. Propellant levels will be monitored to allow for estimation of remaining delta-v available. A radio frequency gauging technique is currently in development that will work at cryogenic temperatures. The pressure before and after all valves and regulators in the propellant feed system will also be monitoring to enable diagnosis of faults. The power system will require monitoring of battery and fuel cell voltages, along with the temperatures and pressures of the oxygen and hydrogen entering the fuel cell system. Data from the suits consisting of heart rate and other physiological parameters will also be relayed to mission control.

Fault Tolerance

The vehicle has been designed to provide two-fault tolerance. It will carry four flight computers, operating in parallel, voting in the event of a discrepancy. Except in the unlikely event of a two-two split, this will allow for identification of up to two failed computers. Redundant wiring will ensure that faults in the command and data handling system do not interfere with use of critical navigational instruments. Navigational instruments were chosen such that the loss of any one device would not cause loss of mission, and the loss of any two devices would still allow a safe return to base. Via ranging to the Lunar Communication Terminals, the vehicle can return to base even in the event of a significant loss of navigational functionality.

Communications

The Constellation architecture as planned by NASA will use Ka-band and S-band for the primary communications links both among surface nodes and between the lunar surface and Earth. For the purposes of this project, it is assumed that the DSN 34 m BWG antennas would be available for a direct-to-Earth communications link with Alshain in both frequency bands. A constellation of lunar relay satellites providing 8 hours of coverage every 12 hours is also assumed to be part of the Constellation architecture for non-line-of-site communications between Alshain and Earth. Stationary surface nodes such as lunar communications terminals (LCTs) may also serve as relays, hubs, and navigational aides that use radiometrics to aid landings in case other navigational hardware, such as LIDAR, fails.

The 26 GHz Ka-band downlink will be capable of at least 100 Mbps and will be used for high-bandwidth mission data such as video or scientific data in addition to LIDAR scans in autonomous and tele-operation modes. The primary high gain antenna (HGA) used to transmit and receive this data will be a 0.66 m diameter parabolic dish mounted on top of the vehicle and will be driven by a traveling wave tube amplifier capable of over 40 W output power. There will also be a backup 3 m dish capable of 30 Mbps that will enable mission success should the primary unit fail. The primary and secondary HGAs will have half power beam widths of approximately 1.2 and 2.7 degrees, respectively, and will both use 2-axis gimbals to achieve a pointing accuracy of +/- 0.0625 degrees. The vehicle will also be capable of receiving a 23 GHz, 1Mbps uplink on either antenna.

The 2.2 GHz S-band downlink will be capable of at least 160 kbps and will be used for critical data such as voice communications, tracking, telemetry and comm, and vehicle and crew status monitoring. This link will use three quadrifilar helix antennas (QHAs), with two mounted on top of the vehicle capable of reaching both to a lunar relay satellite (LRS) and directly to Earth, and the third mounted on the bottom and capable of reaching lunar surface nodes. QHAs were selected for their omnidirectional radiation pattern and their right-hand circular polarization. Each QHA will be capable of receiving a 2.1 GHz, 16kbps uplink.

As an integral part of the lunar architecture, Alshain's communications system must be fully compatible with all other lunar assets and as such will conform to the standards set by NASA and CCSDS. Among the standards under consideration for data exchange among lunar assets are IEEE 802.11 and 802.16e, which would create a WLAN encompassing a wide area around the lunar base. Constellation EVA suits will incorporate 802.16e for real-time data handling in addition to the backup S-band system. Since both 802.16e and 802.11 fall within the S-band region, these links are multiplexed onto the omnidirectional antennas on board the vehicle and could be driven by software defined radio.

In order to conserve bandwidth while ensuring the integrity of vital data, Alshain incorporates a variable-lossless data compression scheme. One such scheme proposed by CCSDS, the compression level is varied dynamically based on the entropy of the data packet being considered. In order to meet the requirement of transmitting at HDTV rates, raw video will be compressed using the MPEG-4 H.264 standard at a level appropriate to the available bandwidth. Alshain's computers are capable of making all such decisions without direct human intervention.

Power, Propulsion, and Thermal

Main Engine System

Design of the Main Engine System (MES) on the Alshain was performed using a combination of thermodynamic relations for an ideal rocket and historical examples of LOX/LH2 engines. Because existing LOX/LH2 engines are much too large for use with a small vehicle, we had to estimate the characteristics of an engine built specifically for this application. The resulting Main Engine System consists of a single 40 kN engine, 100 cm tall by 80 cm in diameter, with an I_{sp} of 400 seconds, expansion ratio of 45:1, a chamber pressure of 2.0 MPa, and weighs 96 kg.

Determining the amount of thrust the system would be capable of was a function of crew safety, minimizing waste of fuel due to gravity drag, and minimizing engine mass. In order to prevent injury to the crew of the Alshain, a maximum acceleration of 2 g's (19.6 m/s^2) was set. Fully fueled at approximately 2500 kg, the Alshain would achieve 2 g's with approximately 49 kN of thrust, which set the upper limit on thrust capability. Gravity drag – the term given to the reduction in ΔV capability of an engine due to the presence of a gravity field – is minimized by increasing thrust to reduce burn time. The amount of fuel required to achieve a given ΔV is dictated by the following relationship:

$$\Delta V = -V_e \ln\left(\frac{m_f}{m_i}\right) - \frac{gV_e}{T}\left(m_i - m_f\right)$$

Where V_e is exit velocity, g is the moon's gravitational acceleration, T is thrust, and m_f and m_i are the final and initial masses, respectively. Combining this with a mass estimating relationship of 2.4 kg per kN of thrust (determined by a linear regression of historical engines), total system mass is minimized with a thrust of 40 kN.

A single engine system was chosen on the basis that multiple engine systems increase the likelihood of an engine failure event. A single 40 kN engine was then analyzed using thermodynamic relations for an ideal nozzle to determine its size and performance characteristics. An expansion ratio of 45:1, which yields an I_{sp} of 400 seconds, was chosen based on a point of diminishing returns from having larger nozzles. The chamber pressure of 2.0 MPa was chosen primarily to minimize the mass of the propellant and pressurant tanks, but also out of nozzle size concerns.

Propulsion Analysis and Tank System

The goal of the propulsion analysis is to find the minimum amount of propellant that the Alshain needs to complete its max round-trip mission distance of 57 kilometers. One of the requirements for the vehicle is that it must be able to use in-situ propellants to operate. For the moon, this means that the Alshain must use liquid oxygen (LOX) as the oxidizer and liquid hydrogen (LH2) as the fuel.

The Alshain has specific ΔV requirements for the max mission distance. Each ballistic hop will take 700 m/s of ΔV and there is an additional glide ΔV of 200 m/s for picking the landing site. This gives a total ΔV of 1600 m/s. In addition, there must be extra fuel added for the PEM fuel cells, the RCS system, and to account for gravity drag (a non-impulsive burn penalty).

Table 11. Fuel Masses

From the mass budget, the approximate inert mass of the vehicle is 1100 kg with a 30% margin. The propulsion analysis is done with this 30% margin added on, so all the propellant values are conservative estimates of what the vehicle will actually need. In addition to this inert mass, the Alshian must also be capable of carrying two astronauts plus additional payload. This additional payload must be equal to at least the weight of an additional astronaut. This gives a total payload requirement of 500 kg. The table to the right shows the fuel breakdown to meet all these requirements.

Fuel Uses	Mass [kg]
Flight	700
RCS	100
Fuel Cells	3
Gravity Drag	137
Total	940

For the tank system, there are several requirements. First and foremost, the tank system has to meet safety requirements; since the Alshain is a small vehicle, the propellant feed system uses pressure tanks. This provides pressure to the propellant storage system. Therefore, for astronaut safety, the tanks must have high safety factors. For low pressure tanks, such as the propellant tanks, a safety factor of two is used, and for high pressure tanks, such as the pressurant tanks, a safety factor of three is used in accordance with NASA standards.

The second requirement is to minimize the mass of the tank system. This includes the mass of the pressure tanks, the pressurant (which is essentially inert mass for the vehicle) and the propellant tanks (not including the propellant as that is a set constant). Several variables contribute to this final mass, such as the number of tanks, their shape, the reliability requirements, and the overall center of gravity shift of the tanks. The number and reliability of the tanks are closely tied. For the shape of the tanks, two options were considered, spherical and cylindrical. The graph below shows that cylindrical tanks are preferable to spherical from a mass perspective, hence spherical is the chosen shape for the propellant tanks. For number of pressure tanks, the bottom right graph shows that around 4 pressure tanks.

The second requirement is to minimize the vehicle volume. This requirement is secondary to minimizing the mass, but it is still an important consideration. Alshain must fit on the deck of the Altair lander, which to the current knowledge of the design team is 6 by 8 meters. Although this is the size of the deck, the vehicle must be significantly smaller than this so that other payloads can be send in addition to the Alshain. For number of pressure tanks, the bottom right graph shows that around four pressure tanks there is a point of diminishing returns for mass. At this point the trade in mass would be minimal in comparison to the increase in volume, hence four pressure tanks were chosen.

Figure 18. Tank Mass Study Histograms

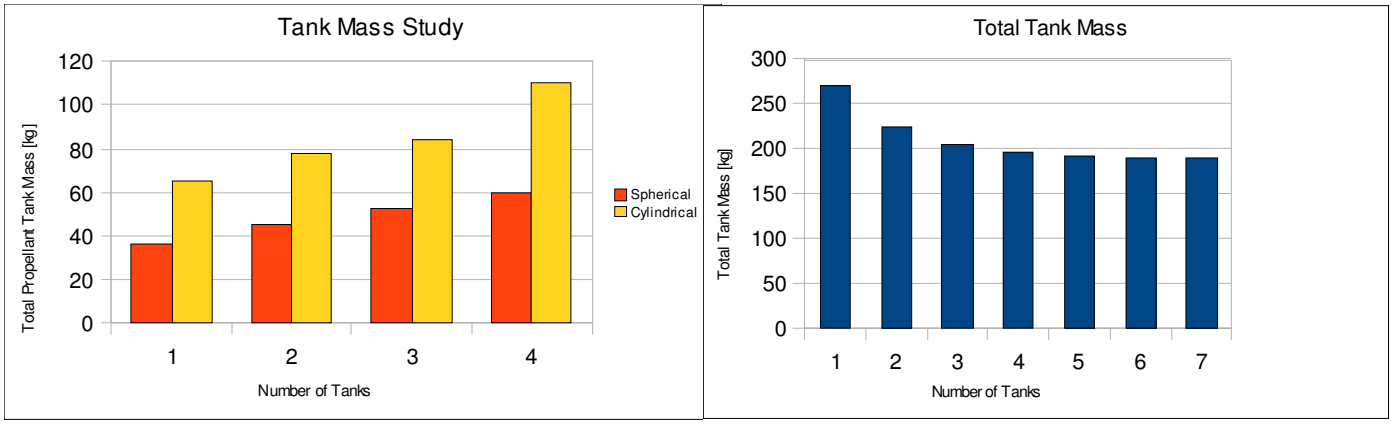

When the system is compiled, the final masses, dimensions and pressures for each aspect of the tank system are as follows:

Table 12. Tank System Statistics

	LOX	LH2	He
Number	2	2	4
Mass of Tank (each) [kg]	9.4	13	31.5
Mass of Propellant/Pressurant (each) [kg]	402	67	10.5
Pressure [Mpa]	2.4	2.4	8.5
Inner Length [m]	NA	NA	0.4
Radius [m]	0.5	0.43	0.45

Reaction Control System

The reaction control system is required to maintain 6 degree of freedom control. It is comprised of 20 thrusters of two different thrusts and 8 mounting locations. These locations were chosen to ensure proper control as well as to protect the astronauts and vehicle from plume impingement from the thrusters. These thrusters maintain control over the worst case scenario center of gravity shifts. Moreover, the RCS system can be used to safely land the vehicle in the event of a main engine failure. Finally, all systems are designed to have two-fault failure tolerance as per NASA requirements.

To maintain the control of the RCS system to all design parameters, the thrust vector of the main engine must always remain under the center of gravity. This means that the vehicle must have sufficient control in pitch (moment about y axis) and roll (moment about x axis). Yaw (moment about the z axis) is not considered in this sense due to the fact that the main thruster is in the x-y plane facing in the downward z direction. Thus, a CG shift in the z direction does not affect the ability of the craft to yaw and would not set a constraint on the design. The maximum CG shift in the x direction is 0.16m and in the y direction is 0.00088m. This equates to a required 6400 Nm pitching torque and a 35 Nm rolling torque.

The factors that affected the thrust requirements were acceleration in all directions, propellant mass flow, size of the thrusters, and mass of the system. Six thrusters plus two spare thrusters (2 fault tolerance) were used in the downward z direction to provide the necessary force to land with appropriate acceleration. At 120 seconds of burn time, the mass of the thrusters versus burn time trend reaches a point of diminishing return, so this was the burn time that was chosen. Since six thrusters must land the vehicle, the mass flow was considered versus the mass flow of the main thruster. Six LOX/LH2 1150N thrusters with a 120 sec burn time use the same amount of propellant as the main 40,000N thruster with a 20 sec burn time.

To maintain attitude control and traversing control in the x and y directions, eight 450N LOX/LH2 thrusters were placed on pods that were boomed out using a triangular space truss structure. The chamber pressure of these thrusters was increased to the maximum system level of 2 MPa to decrease nozzle size and plume expansion to protect astronauts. Below is a summary of the thrusters, RCS placement, and control.

Table 14. Thruster Specifications

Thrust	Mass	Isp	Ve	Mix Ratio	mdot	Po	Ae/At	Length	Diameter
[N]	[kg]	[sec]	[m/s]	[-]	[kg/s]	[Pa]	[-]	[m]	[m]
450	1.08	415	4070	6	0.11	2.00E+06	115	0.067	0.053
1150	2.75	415	4070	6	0.28	2.00E+06	115	0.27	0.21

Table 15. Summary of RCS Thrust and Moment Control

	X Thrust	Y Thrust	Z Thrust	Pitch Moment	Roll Moment	Yaw Moment
	[N]	[N]	[N]	[N-m]	[N-m]	[N-m]
+	900	900	4600	13710	5640	900
-	900	900	9200	13710	5640	900

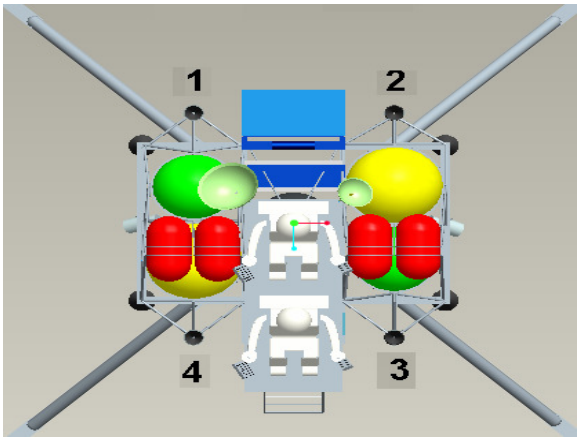

Origin Shown. X is “length” Y is “width”

- Eight 450 N thrusters in x-y plane
  - 2 each on pods 1,2,3,4
  - Pods (±2.13, ±1.0) m
- Eight 1150 N thrusters in ±z direction
  - 2 each on pods 1,2,3,4
  - Pods (±2.13, ±1.0) m
- Four 1150 N thrusters in –z direction
  - Mounted underneath vehicle
  - Mounted (±1.7, ±1.45)

Figure 19. RCS Placement Reference Diagram

Thermal

The thermal control system of the Alshain lunar flying vehicle will have the responsibility of controlling and regulating the temperature of certain subsystems of the vehicle. These subsystems include the seating structure of the astronauts, the avionics box holding the electronics, the fuel cells, and the tanks storing the cryogenic fuels. In order to have a successful mission it is imperative for all systems to operate within their designated temperature ranges. Hence, the thermal control system will make sure these components operate safely during worst-case thermal scenarios. The performance of the thermal control system will be heavily influenced by certain environmental factors. One of the important factors affecting the thermal control system will be the amount of heat flux which is directed towards the system. These heat fluxes include internal power consumed by the electronics and fuel cells, the heat emitted from the astronauts, direct solar radiation from the sun, solar albedo which is solar radiation reflected off of the lunar surface, and also planetary radiation which is the radiation being emitted by the moon itself.

In order to keep the astronaut spacesuits safe from thermal damage, the seating structure of the vehicle must be maintained at a temperature below 320 K. For this matter, the Aeroglaze A276 white paint was chosen. Aeroglaze A276 has the best performance among paints due to its high emissivity of 0.9 and low absorptivity of 0.23. Using this paint, in a worst-case hot scenario, the equilibrium temperature of the seating structure comes down to a safe temperature of 311 K.

The electronics of the lunar flying vehicle are an essential component of the vehicle and must be maintained at safe temperatures during the entire duration of the mission. Table 16 lists the electronics inside the avionics box along with their amount of power consumption. The power consumption of these electronics generates vast amounts of heat inside the avionics box. This heat must be dissipated in order to maintain the electronics at a safe temperature.

Table 16. Avionics Box Electronics

Mass Data Storage	65 W
FPGA/DSP	75 W
IMU	45 W
WLAN	50 W
Flight Computers	100 W
S/Ka Band Transceivers	125 W
Interface Box	75 W
Total with 30% Margin	**695 W**

Flexible optical solar reflectors were chosen to be used as the radiation medium on top of the avionics box. By using the flexible optical solar reflectors, a minimum amount of solar radiation was absorbed, thus lowering the amount of overall heat needed to be dissipated, and thus decreasing the radiation surface area to 2.3 m^2 and a safe equilibrium temperature of 306 K. As mentioned before, the thermal control system must also accommodate for worst-case cold scenarios. During these times there will be only 195 W of internal power consumption which will occur during 24 hour emergency situations. Given the emissivity, absorptivity, and 2.3 m^2 radiation surface area of the optical solar reflectors implemented in the previous section, the equilibrium temperature inside the avionics box reaches 204 K. Therefore, additional adjustments had to be made to raise the temperature to a safe range. The chosen design for this situation is a set of thermal louvers that will be placed on top of the radiation surface area. The main advantage of thermal louvers is that they will permanently be placed on top of the optical solar reflectors and will operate automatically when the need arises. Louvers are thermally activated shutters which require no power to operate, and will open and close based on the temperature of the radiation surface area. Therefore, when the temperature starts to drop in a worst-case cold scenario, the shutters will automatically close. The heat dissipation is then a function of the emissivity of the shutter surfaces in that closed position. Hence, given our surface area which is 2.3 m^2, to maintain a safe equilibrium temperature of 295 K, Aluminum paint with an emissivity of 0.2 will be used for the louver surface finish. Furthermore, a similar system of flexible optical solar reflectors and thermal louvers will regulate the temperature inside the cases holding the fuel cells.

Finally, the cryogenic tanks, namely liquid oxygen and liquid hydrogen, had to be thermally insulated again worst-case hot scenarios. To accomplish this, Aluminized Kapton multi-layer insulation with an effective emissivity of 0.002 was chosen for insulation. An analysis done on the cryogenic tanks, reveals that 1 layer of multi-layer insulation will be enough for each tank. With one layer, the total boil-off from each tank during worst-case hot scenario duration of 32 hours (8 hour mission and 24 hour emergency) will be 0.04 kg for liquid hydrogen and 0.05 kg for liquid oxygen.

Power

The lives of the astronauts and the success of the mission depend on the proper operation of the power system. The Alshain lunar flying vehicle has two fuel cells and two sets of batteries ensuring the delivery of

necessary power even in the worst-case scenario. To better analyze the power requirements, three possible scenarios were created: in-flight, landed at mission site, 24-hour contingency. Table 17 shows the calculations and lists the power draw, duration, and total energy for each scenario.

Table 17. Power System Characteristics

Equipement	**In-Flight (W)**	**Landed (W)**	**Contingency (W)**
Computation & Communication	660	465	170
Propulsion	175 (pulse)	--	--
Control Panels & Lighting	370	90	40
Life Support	--	--	250
Total Power	1030 (1200 pulse)	555	460
With 30% Margin	**1340(1560 pulse)**	**720**	**600**
Duration	6 min.	8 hours	24 hours
Total Energy	**156 (Wh)**	**5760 (Wh)**	**14400 (Wh)**

While in-flight, Alshain demands high power for a short duration of time. Lithium-ion phosphate batteries ($LiFePO_4$) are a type of Li-ion batteries that have high power densities. In a recent publication, this type of battery was found to have specific power exceeding 100kW/kg, power density of 25kW/liter, and, for a half discharge in six minutes, capacity of 160Ah/kg.[13] Using the given specifications, the battery mass required to power Alshain for a round trip of 12 minutes is 3 kg.

When landed, the power system needs to provide 700 Watts to Alshain for 8 hours. During this time, one fuel cell operates, while the other remains on stand-by in case the first fails. NASA has stated that PEM fuel cells will be used in the Constellation Project because the reaction chemistry allows for smaller and lighter systems. [14] Each fuel cell on Alshain operates a stack of 38 individual cells at 28 Volts and 25 Amps, producing 700 Watts of energy at 50% efficiency. The fuel cell measures 20 cm in length, 10 cm in height and width, and weighs 3 kg. Fuel, supplied from the main propulsion feed line, passes through a valve and pressure regulator set to two atm, at which point the large pressure drop causes the fuel to flash vaporize. While still cold, the reactants heat up using 65 Watts of the waste heat from the fuel cell before entering and reacting; the thermal system manages the remaining 635 Watts. Faraday's equation gives the mass flow rate of the reactants as $9.9x10^{-6}$ kg/s for H_2 and $7.9x10^{-5}$ kg/s of O_2; through conservation of mass, the product water mass flow rate is $8.9x10^{-6}$ kg/s. Water is created on the cathode side of the fuel cell and needs to be pushed out so that the fuel cell doesn't drown. Excess oxygen flow, at a stoichiometric ratio of 1.25, pushes the water out of the system; however, this requires the mass flow rate to increase by 25% to $9.8x10^{-5}$ kg/s. An 8-hour mission requires 0.29 kg of H_2, 2.84 kg of O_2, and creates 2.55 kg of water, which along with the extra oxygen, is stored in the water tank.

In the unlikely event that Alshain suffers an accident and cannot return to base, preparations have been made for a 24-hour contingency to allow for crew survival. In this contingency plan, the fuel cells can provide power if there is remaining fuel; 9.4 kg, or rather 1% of the total propellant can provide the necessary 14 kWh. However, there is a possibility that no propellant remains, in which case the fuel cells cannot provide any power. Lithium/Carbon Monoflouride batteries (CFx) are non-rechargeable batteries that have a specific energy of 600 Wh/kg and an energy density of 1100 Wh/liter.[15] To meet the required 14 kWh, Alshain has 24 kg of CFx batteries.

The four power sources connect to a power management and distribution unit (PMAD). The PMAD has control of the fuel cell operation and uses back-boost choppers to ensure that the electronics receive the correct voltage. Furthermore, it acts as an uninterruptible power supply by automatically switching to a working power source in case one fails.

To summarize, Alshain's power system has two sets of batteries and two 700-Watt fuel cells. Table 18 lists the mass estimation for each component.

Table 18. Power System Component Mass

component:	$LiFePO_4$	CFx	Fuel Cells	F.C. Piping	Wiring	PMAD	Total
mass (kg):	3	24	6	4	5	18	60

Mass Budget

The mass budget was maintained with a 30% margin.

Table 19. Mass Budget

Component	Estimate	Margin	Budgeted
LOX Tanks	19 kg	5.7 kg	24.7 kg
LH2 Tanks	26 kg	7.8 kg	33.8 kg
Pressure Tanks	168 kg	50.4 kg	218.4 kg
Rockets/RCS	185 kg	55.5 kg	240.5 kg
Power/Wiring/Thermal	60 kg	18 kg	78 kg
Crew Interfaces/Support	54 kg	16.2 kg	70.2 kg
Lighting/Crew Shielding	47 kg	14.1 kg	61.1 kg
Landing Gear	87 kg	26.1 kg	113.1 kg
Structure	101 kg	30.3 kg	131.3 kg
Avionics	122 kg	32.7 kg	154.7 kg
Reserve		256.8 kg	
Total Inert Mass	869 kg		1125.8 kg

Costing Analysis

Overview and Assumptions

The Alshain Lunar Flying Vehicle was designed to operate as support to the Constellation program. The Constellation program is planned for a return to the moon by 2020 and therefore, the Alshain LFV will be designed to be available for launch in 2020. In order to estimate the expected production and development costs of the Alshain LFV, several assumptions were made. The first assumption is that the Alshain LFV will be capable of being launched on the initial flight of the Ares V in 2020. The second assumption states that a learning curve of 85% was used when calculating recurring production costs. The third assumption is that two Alshain Lunar Flying Vehicles in case of rescue operations on the lunar surface. All of these assumptions were entered in the two NASA Cost Models used to calculate the cost of the Alshain program.

NASA Cost Models

As stated, two NASA Cost Models were used in determining the production and development costs of two Alshain lunar flying vehicles. The first was the NASA Spacecraft/Vehicle Level Cost Model. The second was the NASA Advanced Missions Cost Model. Each model requires input from the user in order to calculate the costs. There are two important inputs in both cost models. The first is the mission type. Neither of these two models currently have a lunar flying vehicle as a selection for the mission type. Therefore, the final production and development costs of the Alshain program are a rough estimate based on the output of each NASA Cost Model. The second is the dry weight. The dry weight is the mass of the vehicle without fuel, consumables, science and research packages, and astronauts. The Alshain LFV dry weight, along with other calculated masses, is shown in Table 19.

Inflation

The two NASA Cost Models output the cost estimates in 2004 dollars. In order to improve the cost estimates, an inflation calculator was used. The inflation calculator accounted for inflation rates and output the cost estimates in 2008 dollars. The inflation calculator is found on the *United States Bureau of Labor Statistics* government website.

Spacecraft/Vehicle Level Cost Model (SVLC Model)

The Spacecraft/Vehicle Level Cost Model takes the following input from the user: program name, mission type, dry weight (pounds or kilograms), quantity, and the learning curve. The mission type is a manned spacecraft because

the Alshain LFV requires astronauts to operate the vehicle. The quantity and the learning curve used in the model are assumptions made for the Alshain LFV.

Advanced Missions Cost Model (AMC Model)

The Advanced Missions Cost Model takes the following input from the user: quantity, dry weight (pounds), mission type, Initial Operating Capability year (initial launch year), block number, and difficulty. The input entered for the Alshain LFV is displayed below:

The quantity remains as stated in the assumptions, two. The dry weight is the same weight used for the SVLC model. The mission type chosen for this model is a lunar rover because the choice of lunar flying vehicle is not available. The Alshain LFV is not a lunar rover; however, a lunar rover is the closest type of mission available for selection. To account for the discrepancy in the mission type, the level of programmatic and technical difficulty (difficulty input) was set to high. The change in the difficulty input should result in a closer estimate of the total cost of the Alshain LFV. The Initial Operating Capability year entered was 2020, the same year listed in the assumptions. The block number represents the level of design inheritance of the vehicle. The block number entered was one because a lunar flying vehicle has never been tested on the lunar surface. The block number and difficulty inputs should adjust for the fact that a lunar rover was chosen as a mission type.

Preliminary Estimate

A preliminary estimate of development and production costs can be made from analyzing the two NASA Cost Models. The preliminary estimate along with costs from each model is shown in Table 20.

Table 20: Preliminary Estimate

Millions FY2008 US$	SVLC Model	AMC Model	Estimate
Development	1,104	745	~900
Production	128	537	~300
Total	1,232	1,282	>1,300

Conclusion

The presumed presence of a replenishable fuel source on the Moon opens up possibilities for lunar flight that would otherwise be economically unfavorable. The characteristics of lunar flight solve the inherent problems found in performing time constrained scientific missions on the Moon. With the exception of some alternatives briefly explored towards the end of the Apollo program, the lunar rover has been the dominant mode of lunar transportation. The lunar flying vehicle provides a significantly more expedient mode of travel than that provided by current rover technology. The Alshain LFV also overcomes the slope and other terrain constraints encountered in rover travel. With the developing plans for lunar research, a lunar flying vehicle is a useful and necessary area of study. The Alshain LFV has been designed to mate with a cargo Altair and is an appropriate complement to the upcoming Constellation program.

Appendix A: Dimensions

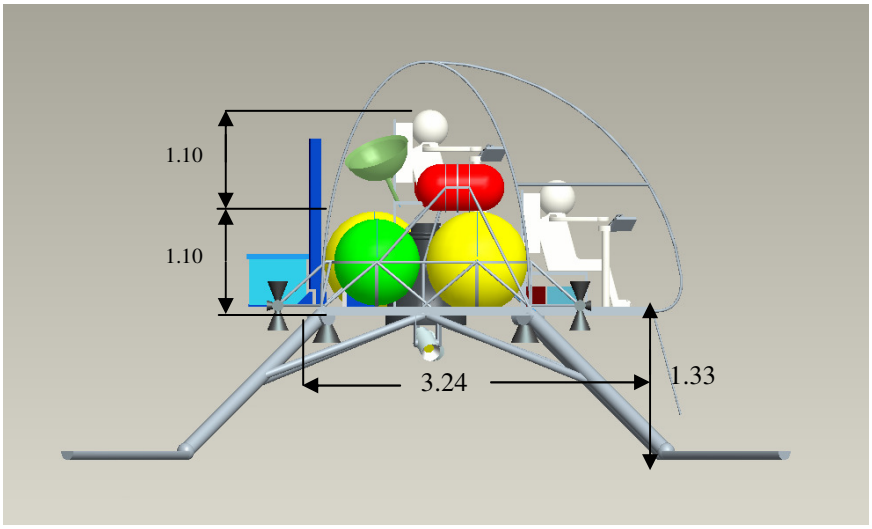

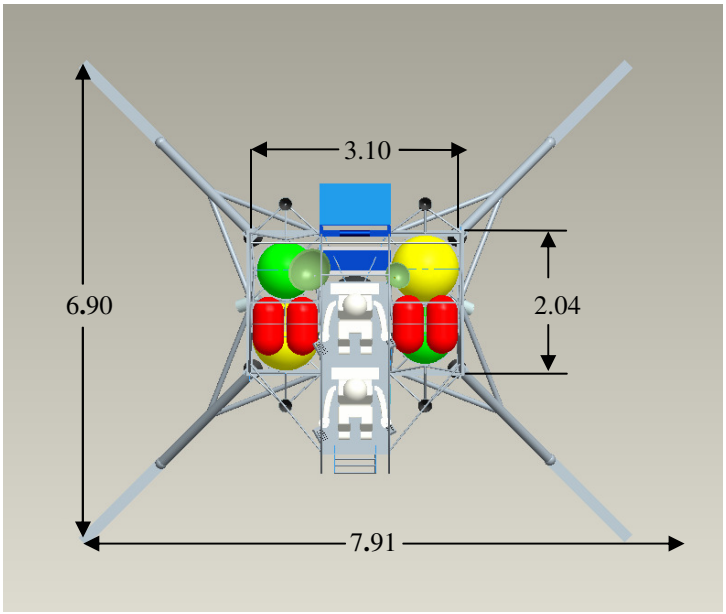

Side and top dimensioned views of the Alshain vehicle:
Note all dimensions are in meters

Appendix B: Moment of Inertia Table

These are the mass moments of inertia for each axis in our nominal Alshain configuration case.

	Pre-flight (kg-m^2)	Post Flight (kg-m^2)
Ixx	*2.41e+003*	*1.26e+003*
Ixy	*-472.5*	*-118.7*
Ixz	*-87.6*	*-87.6*
Iyy	*1.02e+003*	*698.8*
Iyz	*-24.8*	*-24.8*
Izz	*2.19e+003*	*1.03e+003*

Appendix C: Reliability Fault Tree

The following analysis examines the overall system reliability of the Alshain vehicle by creating a system level fault tree. It is analyzed in two different modes: loss of crew, and loss of mission. The top level event of the fault tree in each system is the failure of the Alshain vehicle; however, one is a system level failure that leads to the loss of the mission, while the other is a system level failure that leads to the loss of the crew. It then breaks down by subsystem, and incorporates lower level events that could also lead to total vehicle failure. On the most basic level, reliabilities are assigned to parts based on TRL level and component research. This is an area of high uncertainty that greatly limits the accuracy of the analysis.

Parts List:

The table below summarizes the individual parts that make up the vehicle and their respective reliabilities:

Parts	Number	Reliability
Computer	4	0.9998
HUD	2	0.9999
Fuel Cell	3	0.999
IMU	3	0.9999
Joystick	2	0.9999
Keypad	2	0.9999
Pressurant	4	0.9999
LH2Tank	2	0.9999
LIDAR	1	0.9999
LOX Tank	2	0.9999
Main Thruster	1	0.999
Pres Regulator	11	0.999
RCS Thruster	20	0.999
Radar	1	0.9999
Valve	12	0.999
Main Batteries	1	0.9999
Backup Batteries	1	0,9999

As stated previously, at this stage in the development of the Alshain lunar flying vehicle, component reliabilities are highly speculatory, and limit the overall accuracy of the reliability analysis. That being said, a reliability study of this nature still provides a useful baseline for system reliability as well as an ideal method of subsystem analysis.

Fault Tree Structure:

The following shows an outline of the main fault tree structure. A summary is shown since the actual fault tree is an extremely large and complicated web of subsystems, gates, and conditional faults.

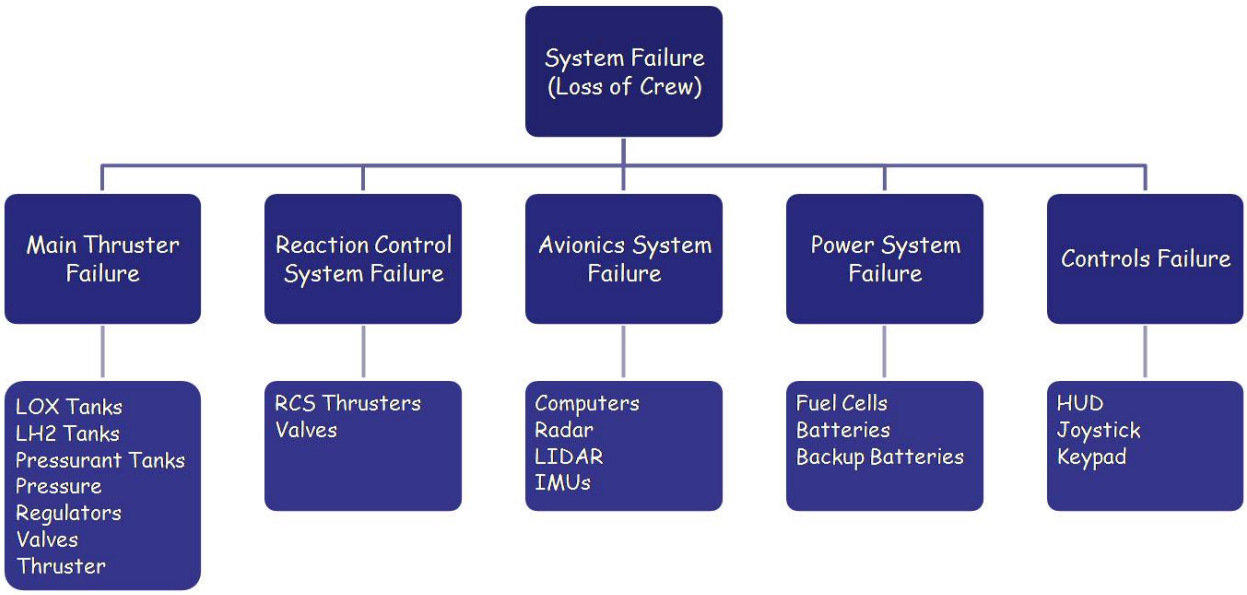

Subsystems

Each of the subsystems shown directly below the top level event in the above summary, represents a critical system that would lead to the loss of crew if it failed during flight operations. In the case of a loss of mission analysis, even minor failures within these critical subsystems that don't cause the systems themselves to fail could lead to the loss of the mission.

This structuring allows for sub analysis of the critical systems individually in order to determine week points at any level within the main system.

Monte Carlo Simulation

These fault trees were developed using the program Open Fault Tree Analysis. This software allows the ability to run fault trees through Monte Carlo simulations to determine the weaknesses of the system as well as the overall system reliabilities.

Early analysis was done by giving all components equal reliabilities in order to locate and analyze single points of failure within the system. This type of analysis had two results:

• It showed the weakness of the propulsion feed system, which led to the restructuring of the pressure regulator and valve scheme as well as the cross feeding of both propellant and pressurant tanks.

• It showed the lack of redundancy in certain areas, which led to the addition of a fourth pressure vessel and additional RCS thrusters.

Results: Loss of Crew

Upon simulation of the fault tree built for loss of crew analysis, a total system reliability of 99.6% is found. The weakest areas leading to this reliability are as follows:

Weak Points	System Failures Caused
RCS Thrusters	27.37%
Pressure Regulators	26.89%
Valves	26.77%

NASA requires a 99.9% system reliability to be achieved prior to use, but this is only the reliability of a very preliminary design. However, we have exposed these areas of component weakness within our analysis that could be used as focus points for future research efforts.

Results: Loss of Mission

Upon simulation of the fault tree built for loss of mission analysis, a total system reliability of 99.2% is found. In this case, the weakest areas leading to this reliability are as follows:

Weak Points	System Failures Caused
RCS Thrusters	27.76%
Main Thruster	14.60%
Fuel Cells	13.72%
Pressure Regulators	13.66%
Valves	13.59%

Appendix D: Crew Workspace and Contingency

Joysticks

The Alshain will employ standard NASA joysticks on the craft. One joystick will be used for control of the translational motion of the Alshain while the other joystick will be used for control of the rotational motion of the Alshain allowing the astronaut to have six degrees-of-freedom control of the craft.

Keypad

The external keypad will be used for all mission-critical tasks on the Alshain. The keypad contains 22 buttons including: 0-9 numerical keys, '+', '-', A-F letter keys, clear, enter, reset, and proceed. The keypad will also have three covered switches for mission abort, engine cut-off, and manual control.

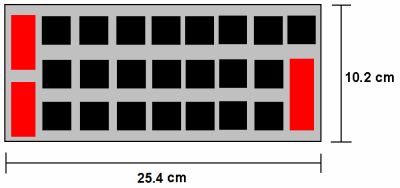

Voice Commands

The voice interface system will be able to give audio feedback to the astronaut through the headset as well as respond to vocal commands given by the astronaut. The voice system will only be used for non-critical tasks.

Heads-up Display (HUD)

The astronaut will be able to monitor all necessary navigation and status data on the craft through a HUD. The HUD is not susceptible to glare issues and is always within the view of the astronaut, so the astronaut will not have to turn away from a point of interest to view displayed information.

Warning Lights

Mission-critical warnings and status lights will be displayed on a light panel attached to the left control stick. The 8 lights and indicators will include master warning, radar fault, low propellant level, restart condition, navigation fault, program fault, PLSS latch engagement, and boot latch engagement.

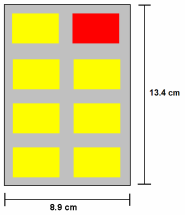

Work Envelope

The control sticks must be placed within reach of both the 5th percentile American female and the 95th percentile American male. NASA tests show that the acceptable controller height is between 28" and 35". Acceptable controller distance in front of the astronaut seat is from 7" to 14". The warning light panel and the keypad are placed within sight range of the astronaut on the control sticks, but they are designed to minimize interference with sight lines.

Hardware

The control panels with a mock light panel and a mock keypad were used in the hardware component of the Alshain vehicle design. None of the controls interfered with ingress/egress of the 'astronaut', and the 'astronaut' was able to easily reach the control sticks. The hardware test resulted in an adjustment of the control panel placement due to lack of access.

Contingency

Each astronaut requires 1.6 kg of drinking water each day. Each astronaut will be supplied with this extra drinking water through a feed tube directly into the helmet. There will be one 0.2 meter diameter tank of water that will supply both astronauts in an emergency. The drinking water will be kept at 20°C with insulation. Each astronaut also needs a total of 15.7 kg of cooling water for a 24 contingency time period. The drinking water tank is 0.15 meters long, 0.34 meters in diameter cylinder with spherical end caps. The oxygen used by the astronauts is supplied by the liquid oxygen oxidizer tanks of the Alshain. Extra oxygen will be drained off the tank, heated using 2 watts per astronaut by the craft power system, and fed through a pressure regulator to reduce the pressure from 348 psi to 4.3 psi. The flow will be regulated by the PLSS flow regulators.

Carbon Dioxide Scrubbing

A total of 2 kg of carbon dioxide needs to be removed from the space suits to prevent poisoning of the astronauts. The air within the space suit will be cycled through the carbon dioxide scrubber using an umbilical. LiOH was chosen as the carbon dioxide scrubber because of its high density.

Power

Each space suit requires 120 watts of power for the period of 24 hours for the fans, pumps, and communications within the suit. The power will be supplied by the Alshain power system fuel cells or auxiliary batteries.

Appendix E: Hardware

The following pictures show a hardware mockup constructed for human factors testing. A suited subject tested ingress and egress procedures.

Appendix F: Error Budget Calculation

Initial attitude error

Initial attitude uncertainty results in traveling in the wrong direction. For a given distance traveled r at an angle θ the resulting position error δ is:

$$\delta = \sqrt{\left(r\sin(\theta)\right)^2 + \left(r\left(1-\cos\left(\theta\right)\right)\right)^2}$$

Accelerometer bias error

Accelerometer bias error results in an unknown, but constant, acceleration being applied to the vehicle at all times. For a given time traveled t with unknown acceleration a_{bias}, the resulting position error δ is:

$$\delta = \frac{1}{2} a_{bias} \cdot t^2$$

Accelerometer scale factor error

Accelerometer scale factor error results in an unknown acceleration being applied to the vehicle that scales linearly with the measured acceleration (zero acceleration being the state of freefall). For a given time traveled t at an average acceleration (magnitude) $\bar{a}$ with an unknown acceleration scale factor a_{sf}, the resulting position error δ is:

$$\delta = \bar{a} \cdot \frac{1}{2} a_{sf} \cdot t^2$$

Gyro bias error

Gyro bias error results in an unknown, but constant, angular velocity being applied to the vehicle at all times. For a given average velocity $\bar{\bar{v}}$ (magnitude) with unknown angular velocity ω_b over a time t, the resulting position error δ is:

$$\delta = \bar{v} \cdot \sqrt{\left(\int \sin(\omega_b t)dt\right)^2 + \left(\int \left(1-\cos\left(\omega_b t\right)\right)dt\right)^2}$$

Gyro scale factor error

Gyro scale factor error results in an unknown angular velocity being applied to the vehicle that scales linearly with the measured angular velocity. For a given average velocity $\bar{\bar{v}}$ (magnitude) with unknown angular velocity scale factor ω_{sf} at an average angular velocity (magnitude) $\bar{\omega}$ over a time t, the resulting position error δ is:

$$\delta = \bar{\omega} \cdot \bar{v} \cdot \sqrt{\left(\int \sin(\omega_{sf} t)dt\right)^2 + \left(\int \left(1-\cos\left(\omega_{sf} t\right)\right)dt\right)^2}$$

Gyro angular random walk

Angular random walk is an error associated with random noise on a measurement. Even if the noise is a zero mean process, the sum at any particular instant is most likely not zero, and so angular random walk is modeled as an unknown angular velocity being applied to the vehicle that varies with the square root of time. For a given average velocity $\bar{v}$ *(magnitude) with unknown angular velocity* ω_{rw} over a time *t*, the resulting position error δ is:

$$\delta = \bar{v} \cdot \sqrt{\left(\int \sin(\omega_{rw}\sqrt{t})dt\right)^2 + \left(\int \left(1 - \cos\left(\omega_{rw}\sqrt{t}\right)\right)dt\right)^2}$$